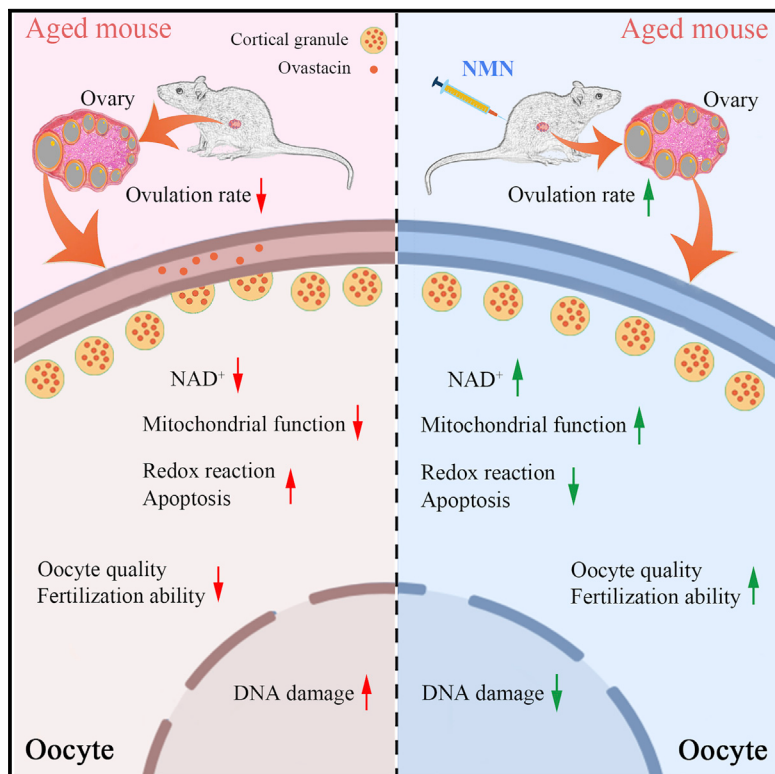


Nicotinamide Mononucleotide Supplementation Reverses the Declining Quality of Maternally Aged Oocytes

Graphical Abstract



Authors

Yilong Miao, Zhaokang Cui, Qian Gao,
Rong Rui, Bo Xiong

Correspondence
xiongbo@njau.edu.cn

In Brief

Miao et al. find that *in vivo* supplementation of the NAD⁺ precursor nicotinamide mononucleotide (NMN) effectively improves the quality of maternally aged oocytes by restoring their mitochondrial function and enhancing meiotic competency, fertilization ability, and subsequent embryonic development potential. This study provides a potential strategy to improve the reproductive outcome of women of advanced maternal age.

Highlights

- NMN supplementation restores NAD⁺ levels in maternally aged oocytes
- NMN increases the number of ovulated oocytes in aged mice
- NMN enhances meiotic competency and fertilization ability of aged oocytes
- NMN recovers mitochondrial function to suppress ROS-induced apoptosis in aged oocytes



Article

Nicotinamide Mononucleotide Supplementation Reverses the Declining Quality of Maternally Aged Oocytes

Yilong Miao,¹ Zhaokang Cui,¹ Qian Gao,² Rong Rui,² and Bo Xiong^{1,3,*}

¹College of Animal Science and Technology, Nanjing Agricultural University, Nanjing 210095, China

²College of Veterinary Medicine, Nanjing Agricultural University, Nanjing 210095, China

³Lead Contact

*Correspondence: xiongbo@njau.edu.cn

<https://doi.org/10.1016/j.celrep.2020.107987>

SUMMARY

Advanced maternal age is highly associated with a decline in oocyte quality, but effective approaches to improve it have still not been fully determined. Here, we report that *in vivo* supplementation of nicotinamide mononucleotide (NMN) efficaciously improves the quality of oocytes from naturally aged mice by recovering nicotinamide adenine dinucleotide (NAD⁺) levels. NMN supplementation not only increases ovulation of aged oocytes but also enhances their meiotic competency and fertilization ability by maintaining the normal spindle/chromosome structure and the dynamics of the cortical granule component ovastacin. Moreover, single-cell transcriptome analysis shows that the beneficial effect of NMN on aged oocytes is mediated by restoration of mitochondrial function, eliminating the accumulated ROS to suppress apoptosis. Collectively, our data reveal that NMN supplementation is a feasible approach to protect oocytes from advanced maternal age-related deterioration, contributing to the improvement of reproductive outcome of aged women and assisted reproductive technology.

INTRODUCTION

High-quality oocytes, a prerequisite for successful fertilization and subsequent embryonic development, is the material basis for onset of life. In most mammals, female reproductive aging is particularly defined by a prominent decline in the quantity and quality of follicles and oocytes (Yamamoto et al., 2010). It has been shown that the fecundity of women begins to drop in the early 30s and declines more rapidly after the age of 35 (Eijkelmans et al., 2014; Tan et al., 2014), accompanied by a dramatically increased incidence of infertility, miscarriage, embryo lethality, and congenital birth defects (Duong et al., 2012; Magnus et al., 2019). Thus, low-quality oocytes are a common and insurmountable problem for women with advanced maternal age and a main cause of suboptimal reproductive outcome (Ciancimino et al., 2014; Heffner, 2004). Despite of the significance of the problem, strategies to sustain oocyte quality with age have been explored poorly.

Nicotinamide adenine dinucleotide (NAD⁺) is an abundant cofactor that participates in multiple aspects of cellular metabolism (Bonkowski and Sinclair, 2016). Recently, the importance of NAD⁺ has expanded from a key element in intermediate metabolism to a critical regulator of diverse physiological processes, such as DNA repair, autophagy, adaptive stress responses, genomic stability, and cell survival (Bonkowski and Sinclair, 2016; Croteau et al., 2017; Kennedy et al., 2016). In particular, it has been reported that NAD⁺ levels decrease with age across many tissues and are implicated in a variety of diseases related

to aging (Bonkowski and Sinclair, 2016). Loss of NAD⁺ alters the NAD⁺/SIRT1 axis and leads to neurodegeneration, vascular inflammation, increased fat storage, increased fat production, insulin resistance, fatigue, and loss of muscle strength (Cantó et al., 2012; Kiss et al., 2020; Scheibye-Knudsen et al., 2014; Yamaguchi and Yoshino, 2017). Therefore, recovery of NAD⁺ levels is likely to be an effective anti-aging intervention. Nicotinamide mononucleotide (NMN), a product of the nicotinamide phosphoribosyltransferase (NAMPT) reaction and a key NAD⁺ intermediate, can reverse defects in mitochondrial homeostasis, reactive oxygen species (ROS) production, DNA repair, as well as cell survival caused by insufficient NAD⁺ (Croteau et al., 2017). Studies have demonstrated that NMN supplementation improves glucose intolerance and lipid profiles in age-induced type 2 diabetes (T2D) mice (Yoshino et al., 2011) and rescues cerebromicrovascular endothelial function as well as neurovascular coupling responses to improve the cognitive function of aged mice (Tartanini et al., 2019). Although great progresses has been made in application of NMN toward aging, the effect of NMN on female reproductive aging has not been fully determined.

In the present study, we discovered that *in vivo* supplementation of NMN restored the NAD⁺ levels in maternally aged oocytes, enhancing their maturation rate, fertilization ability, and subsequent embryonic development potential. By single-cell transcriptome analysis, we further ascertained that NMN supplementation improved the quality of aged oocytes by recovering mitochondrial function, which, in turn, reduced the accumulated ROS to suppress apoptosis during aging.



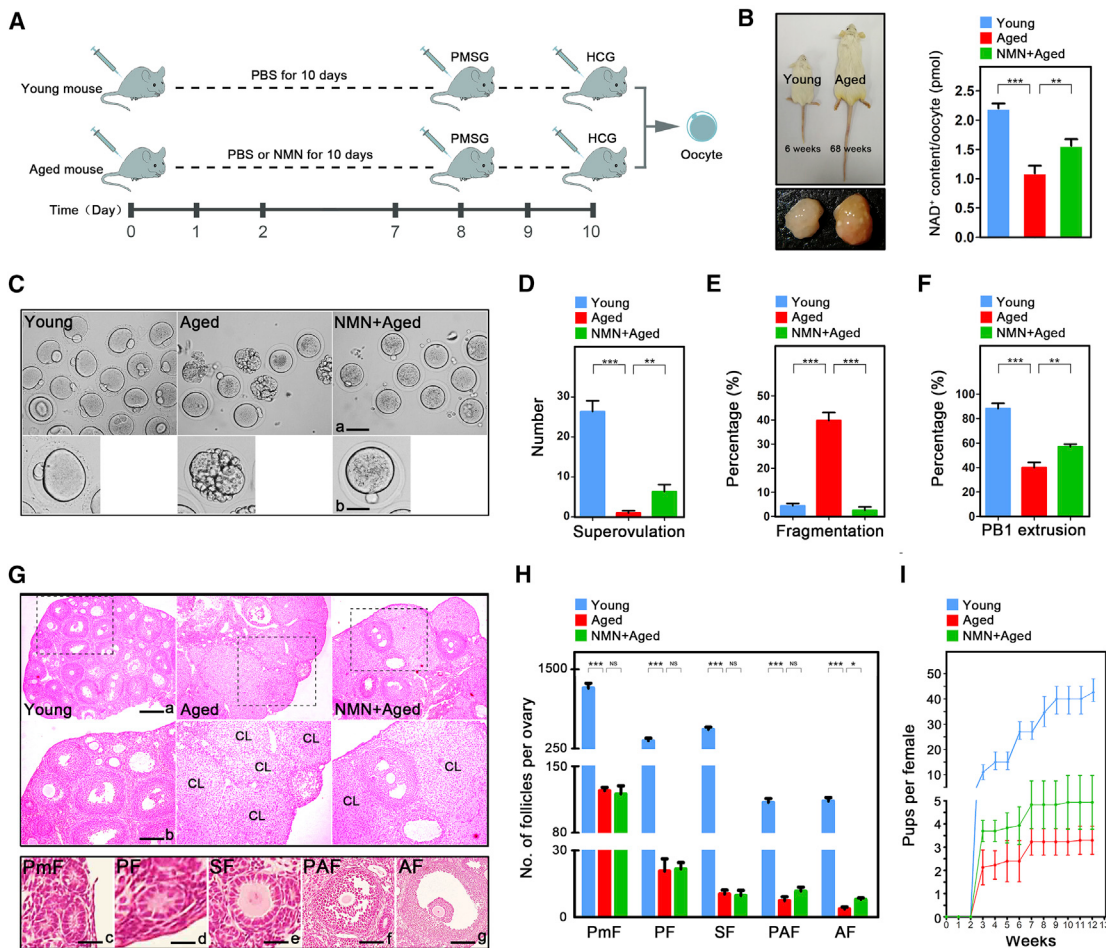


Figure 1. Effect of NMN Supplementation on NAD⁺ Content and Quality of Maternally Aged Oocytes

- (A) A timeline diagram of NMN administration to mice and hormone injection for superovulation of oocytes.
- (B) Representative images of young and aged mice as well as their ovaries. NAD⁺ levels were measured in young, aged, and NMN+aged oocytes (n = 80 for each group).
- (C) Representative images of *in-vivo*-matured oocytes collected from young, aged, and NMN+aged mice. Scale bars: a, 80 μm; b, 40 μm.
- (D) Ovulated oocytes were counted in young (n = 5), aged (n = 5), and NMN+aged (n = 5) mice.
- (E) The rate of first PBE was recorded in young (n = 21), aged (n = 19), and NMN+aged (n = 20) oocytes.
- (F) The rate of fragmented oocytes was recorded in young (n = 24), aged (n = 21), and NMN+aged (n = 23) groups.
- (G) Representative images of ovarian sections from young, aged, and NMN+aged mice. Ovaries were embedded in paraffin, and sections of 8-μm thickness were prepared and stained with H&E. Scale bars: a, 250 μm; b, 50 μm; c, 10 μm; d, 20 μm; e, 50 μm; f, 120 μm; g, 150 μm. PmF, primordial follicle; PF, primary follicle; SF, secondary follicle; PAF, pre-antral follicle; AF, antral follicle; CL, corpus luteum.
- (H) Follicles at different developmental stages were counted in young (n = 6), aged (n = 6), and NMN+aged (n = 6) ovaries.
- (I) The fertility of young (n = 6), aged (n = 6), and NMN+aged (n = 6) female mice was assessed by mating with young male mice and recording the cumulative number of pups born over time for 12 weeks.
- Data in (B), (D)–(F), (H), and (I) are presented as mean percentage (mean ± SEM) of at least three independent experiments. *p < 0.05, **p < 0.01, ***p < 0.001.

RESULTS

NMN Supplementation Improves the Quality of Aged Oocytes by Increasing NAD⁺ Content

We first investigated whether NMN supplementation would restore the NAD⁺ content in oocytes from maternally aged mice. Young and aged mice were administered PBS or NMN for 10 consecutive days and received hormones on days 8 and 10 for superovulation (Figure 1A). To determine the optimal dose, different concentrations of NMN (50, 100, 200, 500, and 1,000 mg/kg body weight/

day) were administered to obtain mature oocytes. The highest number of mature oocytes was obtained from aged mice at doses of 200 and 500 rather than 1,000 mg/kg body weight/day of NMN (Figure S1). Given that a previous studies reported that local NMN accumulation because of administration of high doses of NMN might have negative effects on tissues and cells (Mills et al., 2016; Park et al., 2016), we then used a dose of 200 mg/kg body weight/day for our subsequent study. As expected, a significant decrease in NAD⁺ levels was detected in aged oocytes compared with young ones (Figure 1B). In contrast, administration of NMN in

aged mice remarkably elevated the NAD⁺ content in oocytes, indicating that NMN supplementation might be a potential strategy to improve the quality of aged oocytes. To test this, we evaluated the oocyte morphology of young, aged, and NMN+aged mice. We found that maternal aging dramatically reduced the number of ovulated oocytes and the rate of matured oocytes but increased the incidence of fragmented oocytes (Figures 1C–1F). Conversely, NMN supplementation apparently ameliorated the defects in the number and morphology of oocytes caused by aging. In addition, we assessed follicle development by ovary sections. We observed severe deterioration of follicles at different developmental stages in aged mice, and NMN supplementation increased the number of antral follicles to some extent (Figures 1G and 1H), supporting the result that ovulated oocytes from aged mice grew in number following NMN supplementation. The reason why only antral follicles were recovered by NMN might be the short-term acute NMN treatment in the current study. Long-term NMN supplementation might have better effects on other developmental stages of growing follicles. Consistent with the increased number of mature oocytes with normal morphology, the fertility of aged mice was also improved by NMN administration (Figure 1I). It is notable that the number of pups in aged mice after NMN supplementation only significantly increased at the first litter, suggesting that the effect of short-term acute NMN supplementation for 10 days on aged oocytes in our study lasted no more than 1 month. Furthermore, we did not observe any developmental abnormalities, as assessed by body and organ weight, in both sexes of pups from young, aged, and NMN+aged mice (Figure S2). Thus, these observations indicate that NMN can partially restore the number and morphology of aged oocytes by enhancing NAD⁺ levels, improving the fertility of the animals.

NMN Supplementation Recovers Meiotic Maturation of Aged Oocytes

Germinal vesicle (GV) oocytes isolated from young, aged, and NMN+aged mice were cultured *in vitro* to determine how NMN improves oocyte maturation ability. Quantification of the first polar body extrusion (PBE) rate revealed that meiotic progression was impaired in aged oocytes but recovered in NMN-supplemented aged oocytes (Figures 2A and 2B). Because meiotic arrest was mainly due to defective spindle/chromosome structure, we further examined it in oocytes from three groups. As assessed by immunostaining images, a variety of disorganized spindle apparatuses with misaligned chromosomes were present in aged oocytes at the metaphase I and metaphase II stages (Figure 2C). The quantitative data showed that the occurrence of aberrant spindle/chromosome structure was considerably higher in aged oocytes compared with controls but declined after NMN supplementation (Figures 2D and 2E). These results suggest that NMN is able to effectively improve the maturation ability of aged oocytes by maintaining the correct spindle/chromosome structure.

NMN Supplementation Restores Kinetochore-Microtubule Attachment to Ensure Euploidy in Aged Oocytes

Aberrant spindle assembly and incorrect chromosome alignment are highly correlated with defective attachment between ki-

netochores and microtubules, leading to aneuploidy. We thus tested the effects of NMN on them in aged oocytes. For this purpose, metaphase I oocytes were briefly chilled to induce depolymerization of microtubules that were not attached to kinetochores and then immunostained with calcinosis, Raynaud phenomenon, esophageal dysmotility, sclerodactyly, and telangiectasia (CREST) antibody to detect kinetochores, with an anti- α -tubulin-fluorescein isothiocyanate (FITC) antibody to visualize microtubules, and counterstained with Hoechst to observe chromosomes. In a large number of young oocytes, kinetochores were fully attached to microtubules, and chromosomes were well aligned (Figures 2F and 2G). However, a prominently increased incidence of free kinetochores without attachment to microtubule fibers was observed in aged oocytes but significantly reduced by NMN supplementation (Figures 2F and 2G).

Because impaired kinetochore-microtubule attachment is often coupled with aneuploidy, we then analyzed the karyotype of metaphase II oocytes by chromosome spreading. Normally, the number of chromosomes (univalents) is 20, which is a prerequisite for genomic integrity (Figures 2H and 2I). In contrast, a remarkably higher frequency of aneuploid oocytes that had more or less than 20 univalents was found in aged oocytes compared with young ones, and NMN supplementation, as expected, decreased the aneuploidy rate in the aged group (Figures 2H and 2I). We conclude from these observations that NMN supplementation could promote nuclear maturation of aged oocytes.

NMN Supplementation Rescues the Distribution of Cortical Granules and Ovastacin in Aged Oocytes

Cortical granules (CGs) are oocyte-specific vesicles located under the subcortex to block polyspermy following fertilization. It is noteworthy that the distribution of CGs is usually regarded as one of the most important indicators of oocyte cytoplasmic maturation. We assessed whether NMN would affect the dynamics of CGs in aged oocytes. As judged by *Lens culinaris* agglutinin (LCA)-FITC staining, CGs distributed evenly in the oocyte subcortical region, except the CG-free domain (CGFD) near chromosomes in young oocytes, but lost this normal localization because of discontinuous and weak signals in aged oocytes (Figures 3A and 3B). In line with this, the fluorescence intensity of CG signals in aged oocytes was significantly reduced compared with young ones (Figures 3A and 3C). The mis-localization and decrease in the amount of CGs were rescued by NMN supplementation (Figures 3A–3C).

As the first identified component of CGs in mammals, ovastacin is responsible for post-fertilization cleavage of sperm binding site zona pellucida glycoprotein 2 (ZP2) in oocytes to block additional sperm binding and polyspermy. We observed the same dynamics of ovastacin as for CGs in young, aged, and NMN+aged oocytes (Figures 3D–3F). In addition, the protein level of ovastacin was reduced in aged oocytes but recovered following NMN supplementation, as judged by immunoblot analysis (Figure 3G), indicating that ovastacin might be prematurely exocytosed to the extracellular space of oocytes to impair sperm binding and fertilization of aged oocytes, and NMN supplementation may prevent this to recover oocyte cytoplasmic maturation.

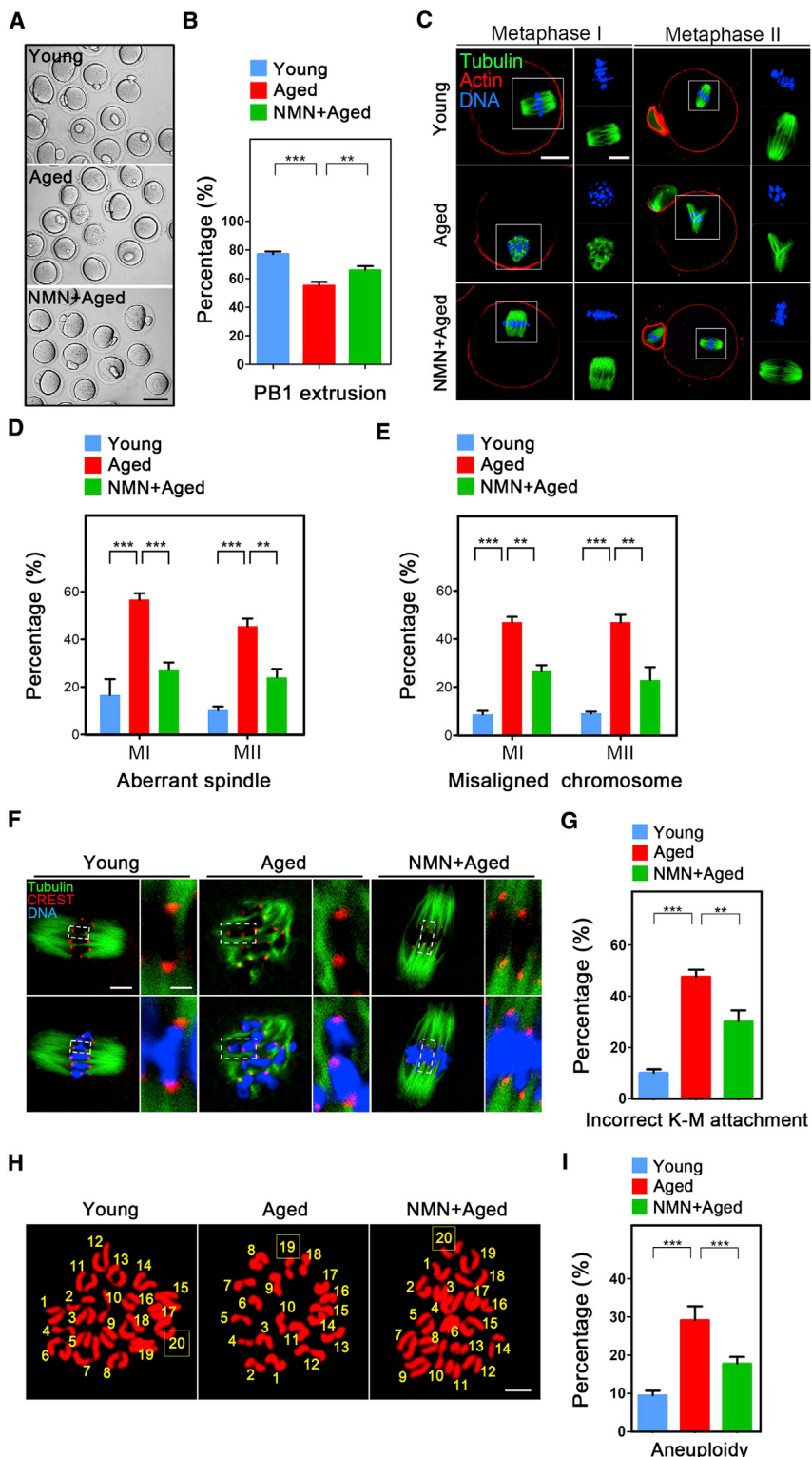


Figure 2. Effect of NMN Supplementation on Meiotic Maturation and Spindle/Chromosome Structure in Aged Oocytes

(A) Representative images of matured oocytes cultured *in vitro* from young, aged, and NMN+aged GV oocytes. Scale bar, 80 μ m.

(B) The rate of first PBE was recorded in young ($n = 39$), aged ($n = 37$), and NMN+aged ($n = 33$) oocytes after maturation for 12 h *in vitro*.

(C) Representative images of the spindle morphology and chromosome alignment at metaphase I and metaphase II in young, aged, and NMN+aged oocytes. Oocytes were immunostained with the α -tubulin-FITC antibody to display the spindles and counterstained with Hoechst to visualize the chromosomes. Scale bars, 20 μ m, 10 μ m.

(D) The rate of aberrant spindles at metaphase I and metaphase II was recorded in young (metaphase I, $n = 27$; M II, $n = 25$), aged (M I, $n = 23$; M II, $n = 21$), and NMN+aged (M I, $n = 25$; M II, $n = 21$) oocytes.

(E) The rate of misaligned chromosomes was recorded in young (M I, $n = 27$; M II, $n = 25$), aged (M I, $n = 23$; M II, $n = 21$), and NMN+aged (M I, $n = 25$; M II, $n = 21$) oocytes.

(F) Representative images of kinetochore-microtubule (K-M) attachment in young, aged, and NMN+aged oocytes. Oocytes were immunostained with an α -tubulin-FITC antibody to show the spindles, with CREST to visualize the kinetochores and counterstained with Hoechst to display the chromosomes. Scale bars, 5 μ m, 2 μ m.

(G) The rate of defective K-M attachment was recorded in young ($n = 17$), aged ($n = 14$), and NMN+aged ($n = 13$) oocytes.

(H) Representative images of euploid and aneuploid oocytes. Chromosome spreading was performed to count the chromosomes in young, aged, and NMN+aged oocytes. Scale bar, 5 μ m.

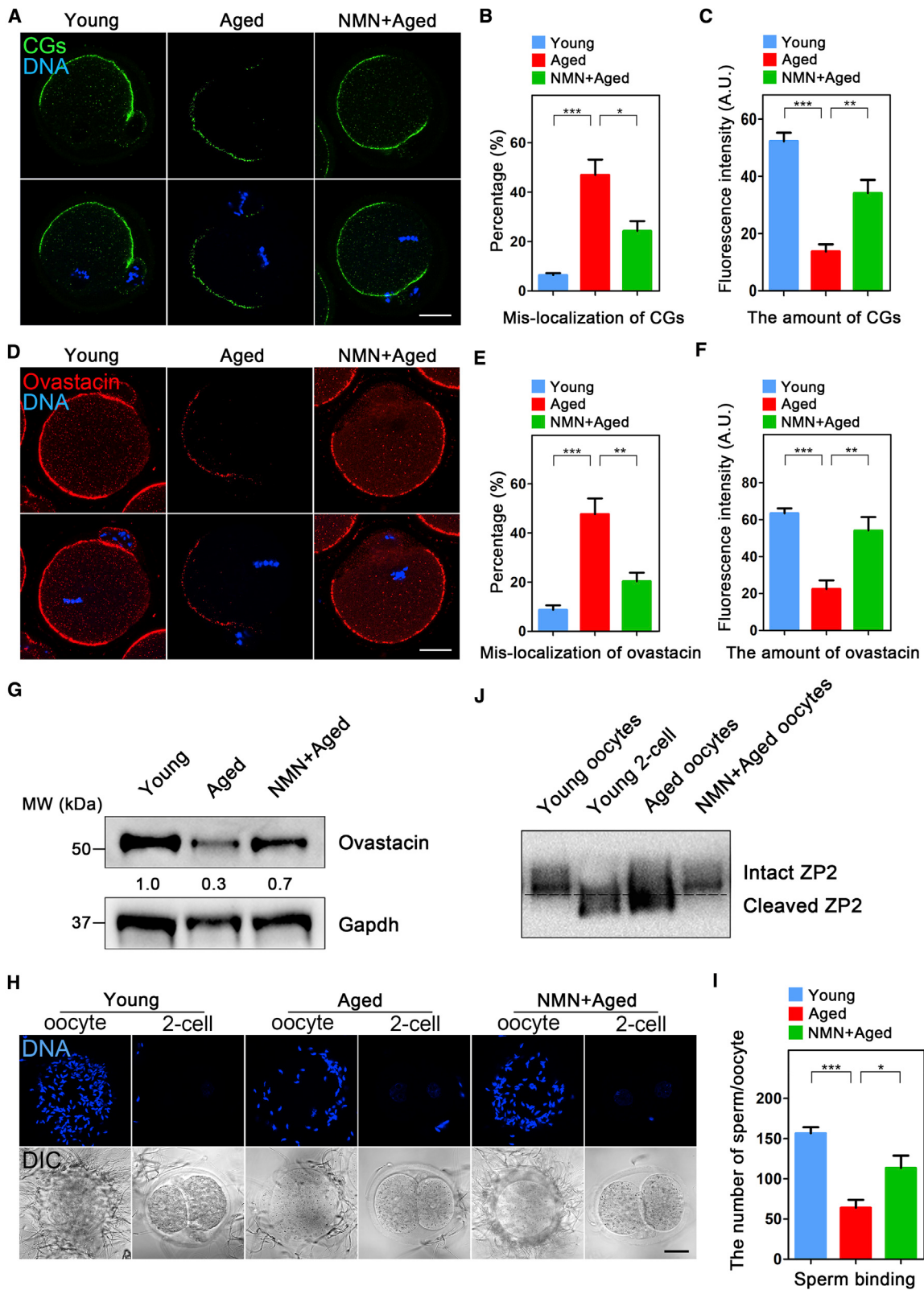
(I) The rate of aneuploidy was recorded in young ($n = 15$), aged ($n = 14$), and NMN+aged ($n = 16$) oocytes. Data in (B), (D), (E), (G), and (I) are presented as mean percentage (mean \pm SEM) of at least three independent experiments. ** $p < 0.01$, *** $p < 0.001$.

performed a sperm-oocyte binding assay followed by staining the sperm head with Hoechst to count the number of sperm binding to the *zona pellucida*. In unfertilized oocytes from young mice, the *zona pellucida* supported robust sperm binding. After fertilization, because of loss of the sperm binding site, the *zona pellucida* no longer supported additional sperm binding in 2-cell embryos (Figures 3H and 3I). In aged oocytes, the number of sperm binding to the *zona pellucida* was remarkably lowered compared with young ones (Figures 3H and 3I) but significantly increased upon NMN supplementation (Figures 3H and 3I).

Because sperm binding ability is dependent on ZP2 cleavage status by ovastacin, we next examined it to verify the result of the

NMN Supplementation Strengthens the Sperm Binding Ability of Aged Oocytes

To validate the possibility that NMN might rescue the sperm binding ability of aged oocytes and improve the fertilization rate, we



(legend on next page)

sperm-oocyte binding assay. Oocytes and/or 2-cell embryos from different groups were immunoblotted with the M2c.2 antibody which recognizes the C terminus of mouse ZP2. In the young group, we observed that ZP2 remained intact around 120 kD in oocytes and became cleaved about 90 kD in 2-cell embryos (Figure 3J). In contrast, the cleaved ZP2 band was present even in unfertilized aged oocytes (Figure 3J), suggesting that the sperm binding site is lost prior to fertilization during aging. The cleavage level of ZP2 in aged oocytes was improved following NMN supplementation (Figure 3J). Therefore, these data show that NMN restores ZP2 integrity from premature cleavage during aging to maintain the sperm binding ability.

NMN Supplementation Improves the Fertilization Ability and Early Embryo Development of Aged Oocytes

We then tested whether the fertilization capacity of aged oocytes supplemented with NMN would be enhanced. An *in vitro* fertilization experiment showed that most young oocytes could be fertilized and developed into 2-cell embryos, whereas aged oocytes had dramatically lower fertilization compared with young ones (Figures 4A and 4B). As expected, NMN supplementation effectively increased the fertilization rate of aged oocytes (Figures 4A and 4B). We further monitored the subsequent early embryonic development of fertilized oocytes, revealing that NMN supplementation markedly promoted the blastocyst formation rate of fertilized oocytes from aged mice (Figures 4A and 4C–4F). These results demonstrate that NMN improves the fertilization ability of aged oocytes and promotes their subsequent embryonic development.

Identification of Target Effectors of NMN in Aged Oocytes by Single-Cell Transcriptome Analysis

To further dissect the underlying mechanisms of the effects of NMN supplementation on the quality of aged oocytes, we performed single-cell transcriptome analysis of ovulated oocytes from young, aged, and NMN+aged mice. The expression of several randomly selected genes in each group was verified using quantitative real-time PCR (Figure S3). Heatmap and volcano plot data reflected that the transcriptome profile of aged oocytes was apparently different from that of young oocytes, showing that 179 differentially expressed genes (DEGs) were downregulated and

344 DEGs were upregulated in aged oocytes (Figures 5A, 5B, and S3; Table S2). In addition, NMN supplementation displayed 66 upregulated DEGs and 61 downregulated DEGs in comparison with aged oocytes (Figures 5A, 5C, and S3; Table S3) as well as 115 upregulated DEGs and 72 downregulated DEGs in comparison with young oocytes (Figures 5A and S3; Table S4).

Kyoto Encyclopedia of Genes and Genomes (KEGG) analysis of DEGs revealed that genes enriched in the oxidative phosphorylation pathway were abnormally expressed in aged oocytes compared with young ones but recovered in NMN+aged oocytes (Figures 5D and 5E). In addition, we noticed that the peroxisome proliferator-activated receptor (PPAR) signaling pathway and several viral infection pathways were changed considerably in NMN+aged oocytes compared with aged and young ones (Figures 5E and S4A), indicative of the anti-inflammatory effects of NMN. Also, Gene Ontology (GO) analysis showed that genes associated with the mitochondrial membrane part, mitochondrial respiratory chain, microtubule, spindle, and DNA repair were misexpressed in aged oocytes but restored after NMN supplementation (Figures 5F, 5G, and S4B). Collectively, all of these pathways or biological processes are highly related to mitochondrial function, which prompts us to focus on mitochondria as NMN effectors in aged oocytes.

NMN Supplementation Restores Mitochondrial Function in Aged Oocytes

To verify the effect of NMN supplementation on mitochondrial function in aged oocytes, we first observed the distribution pattern of mitochondria by MitoTracker staining. We observed that two features of mitochondrial distribution emerged in young oocytes, including accumulated distribution in the periphery of chromosomes and homogeneous distribution in the cytoplasm (Figure 6A). In aged oocytes, however, a great number of mitochondria partially or completely lost their accumulation around chromosomes and presented absent or aggregated distribution in the cytoplasm (Figure 6A). Quantitatively, more than 40% of aged oocytes exhibited the mislocalized mitochondria, and NMN supplementation reduced this to 24% (Figure 6B).

The abnormal distribution of mitochondria indicates that their function might be compromised with aging in oocytes. Given

Figure 3. Effect of NMN Supplementation on the Dynamics of CGs and Ovastacin as well as Sperm Binding Ability in Aged Oocytes

- (A) Representative images of CG distribution in young, aged, and NMN+aged oocytes. CGs were stained with LCA-FITC and imaged by confocal microscope. Scale bar, 20 μ m.
 - (B) The rate of mislocalized CGs was recorded in young ($n = 21$), aged ($n = 19$), and NMN+aged ($n = 17$) oocytes.
 - (C) The fluorescence intensity of CG signals was measured in young ($n = 21$), aged ($n = 19$), and NMN+aged ($n = 17$) oocytes.
 - (D) Representative images of ovastacin distribution in young, aged, and NMN+aged oocytes. Oocytes were immunostained with an anti-mouse ovastacin antibody and imaged by confocal microscope. Scale bar, 20 μ m.
 - (E) The rate of mislocalized ovastacin was recorded in young ($n = 16$), aged ($n = 12$), and NMN+aged ($n = 15$) oocytes.
 - (F) The fluorescence intensity of ovastacin was measured in young ($n = 16$), aged ($n = 12$), and NMN+aged ($n = 15$) oocytes.
 - (G) Protein levels of ovastacin in young, aged, and NMN+aged oocytes. 50 oocytes for each group were collected and immunoblotted for ovastacin and glyceraldehyde-3-phosphate dehydrogenase (Gapdh).
 - (H) Representative images of sperm binding to the zona pellucida of young, aged, and NMN+aged oocytes. Oocytes and 2-cell embryos from young, aged, and NMN+aged mice were incubated with capacitated sperm for 1 h. After washing with a wide-bore pipette to remove all but 2–6 sperm on normal 2-cell embryos (negative control), oocytes and embryos with sperm were fixed and stained with Hoechst 33342. Scale bar, 20 μ m.
 - (I) The sperm binding to the surface of the zona pellucida surrounding oocytes from young ($n = 14$), aged ($n = 12$), and NMN+aged ($n = 12$) groups were counted.
 - (J) ZP2 cleavage status was examined by immunoblot analysis. Oocytes and 2-cell embryos collected from young, aged, and NMN+aged mice were immunoblotted for the C-terminal domain of ZP2 using the M2c.2 antibody. The size of intact ZP2 is 120 kD, and the cleaved fragment is 90 kD.
- Data in (B), (C), (E), (F), and (I) are presented as mean percentage (mean \pm SEM) of at least three independent experiments. * $p < 0.05$, ** $p < 0.01$, *** $p < 0.001$.

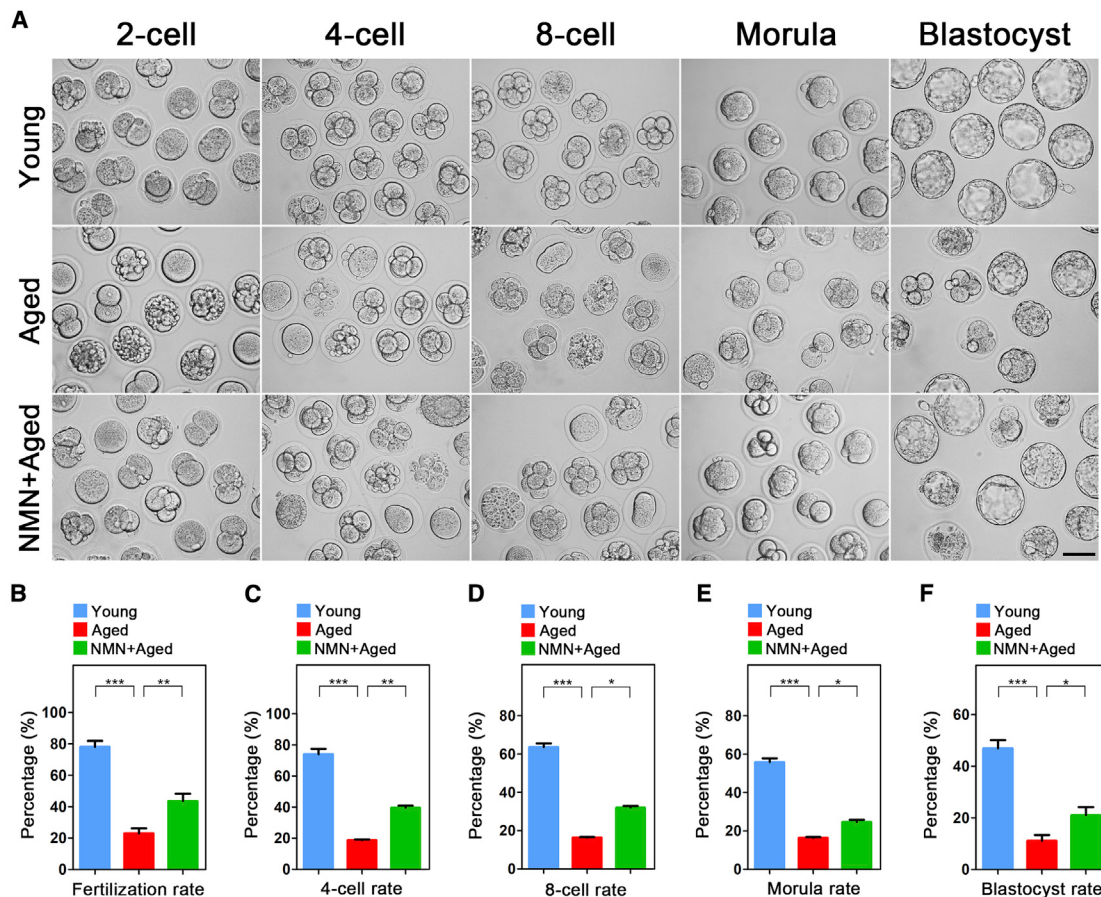


Figure 4. Effect of NMN Supplementation on the Fertilization Ability and Embryonic Development of Aged Oocytes

- (A) Representative images of early embryos developed from young, aged, and NMN+aged oocytes. Scale bar, 100 μ m.
- (B) The fertilization rate was recorded in the young ($n = 22$), aged ($n = 19$), and NMN+aged ($n = 20$) groups.
- (C) The rate of 4 cell embryos was recorded in the young ($n = 21$), aged ($n = 16$), and NMN+aged ($n = 18$) groups.
- (D) The rate of 8 cell embryos was recorded in the young ($n = 20$), aged ($n = 16$), and NMN+aged ($n = 17$) groups.
- (E) The rate of morula was recorded in the young ($n = 18$), aged ($n = 16$), and NMN+aged ($n = 17$) groups.
- (F) The rate of blastocyst formation was recorded in the young ($n = 17$), aged ($n = 15$), and NMN+aged ($n = 13$) groups.

Data in (B)–(F) are presented as mean percentage (mean \pm SEM) of at least three independent experiments. * $p < 0.05$, ** $p < 0.01$, *** $p < 0.001$.

that the most important function of mitochondria is to produce ATP for cell development, we measured the ATP content in oocytes from young, aged, and NMN+aged mice. In agreement with previous studies showing that the aggregation of mitochondria caused by impaired mitochondrial dynamics (aging or genetic ablation of Mitofusin1) compromises mitochondrial function and, thus, reduces ATP production (Ben-Meir et al., 2015; Hou et al., 2019), our results showed that ATP levels declined prominently in aged oocytes compared with young ones but recovered following NMN supplementation (Figure 6C). We then assessed the mitochondrial membrane potential ($\Delta\Psi_m$), the driving force of mitochondrial ATP synthesis, by JC-1 staining. Mitochondria with high membrane potential presented red fluorescence, whereas those with low membrane potential exhibited green fluorescence (Figure 6D). The ratio of red to green signal was much weaker in aged oocytes than in young oocytes but rescued in NMN-supplemented aged oocytes (Figure 6E). We also examined the expression

of genes regulating mitochondrial fusion (*Opa1*, *Mfn1*, and *Mfn2*) and fission (*Drp1*) and found that they were all misexpressed in aged oocytes but restored to a level comparable with young ones after NMN supplementation (Figure 6F). Altogether, these observations suggest that aging-induced mitochondrial dysfunction in oocytes could be improved with NMN supplementation.

Because Sirt1 is a critical regulator of mitochondrial biogenesis and activated by NAD⁺, we next asked whether Sirt1 was involved in restoration of meiotic defects in aged oocytes by NMN. We found that the protein level of Sirt1 was remarkably reduced in aged oocytes compared with young ones but elevated after NMN supplementation (Figure S5A). More importantly, inhibition of Sirt1 activity in NMN+aged oocytes with its specific inhibitor EX527 completely suppressed recovery of meiotic progression and spindle/chromosome structure by NMN supplementation (Figures S5B–S5F), indicating that Sirt1 mediates NMN effects on aged oocytes.

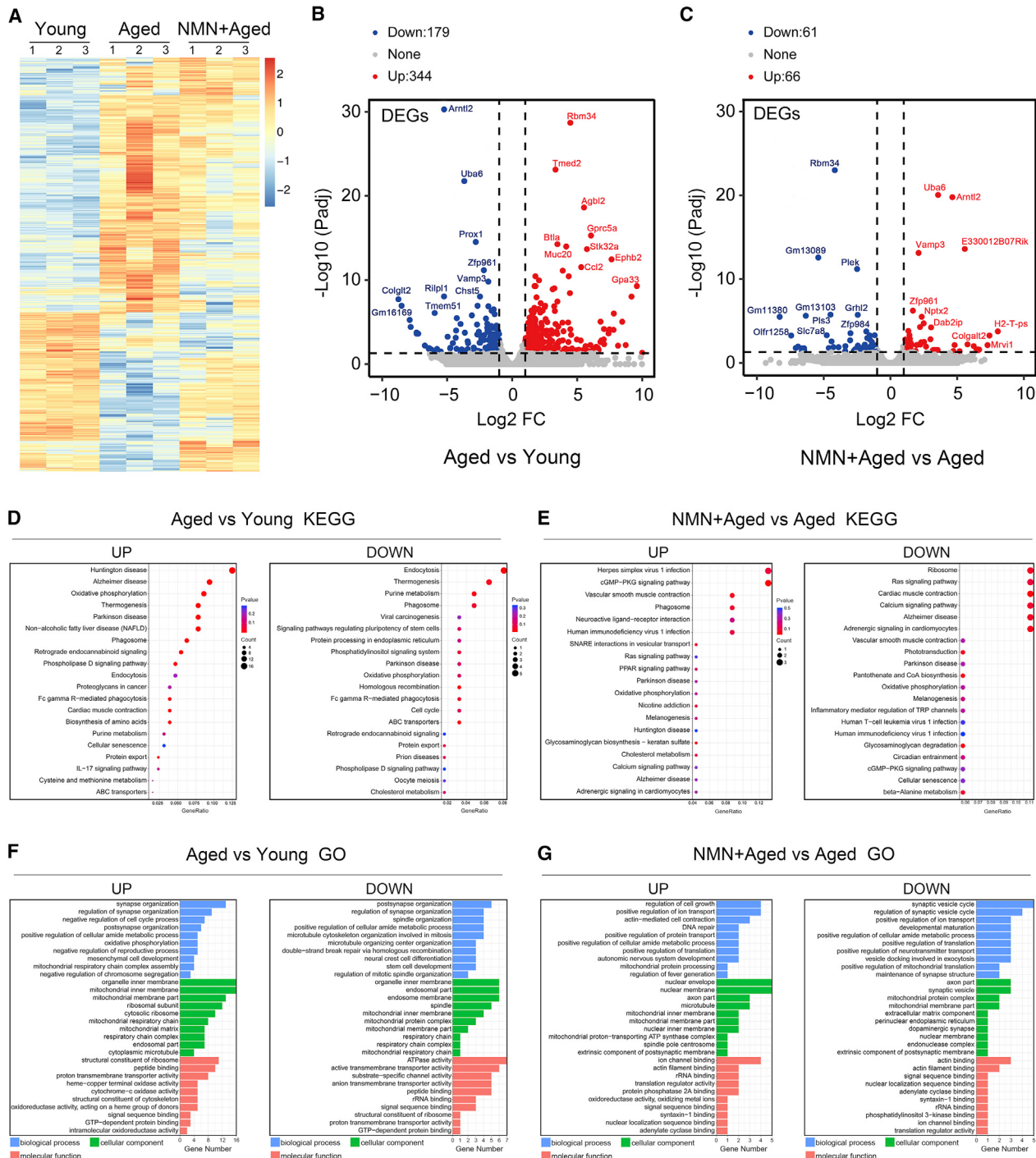


Figure 5. Effect of NMN Supplementation on Transcriptome Profiling of Aged Oocytes

(A) Heatmap illustration displaying gene expression of young, aged, and NMN+aged oocytes.

(B) Volcano plot showing differentially expressed genes (DEGs; downregulated, blue; upregulated, red) in aged oocytes compared with young ones. Some highly DEGs are listed.

(C) Volcano plot showing DEGs (downregulated, blue; upregulated, red) in NMN+aged oocytes compared with aged ones. Some highly DEGs are listed.

(D) KEGG enrichment analysis of upregulated and downregulated DEGs in aged oocytes compared with young ones.

(E) KEGG enrichment analysis of upregulated and downregulated DEGs in NMN+aged oocytes compared with aged ones.

(F) GO enrichment analysis of upregulated and downregulated DEGs in aged oocytes compared with young ones.

(G) GO enrichment analysis of upregulated and downregulated DEGs in NMN+aged oocytes compared with aged ones.

Blue represents biological processes, green represents cellular components, and orange represents molecular function.

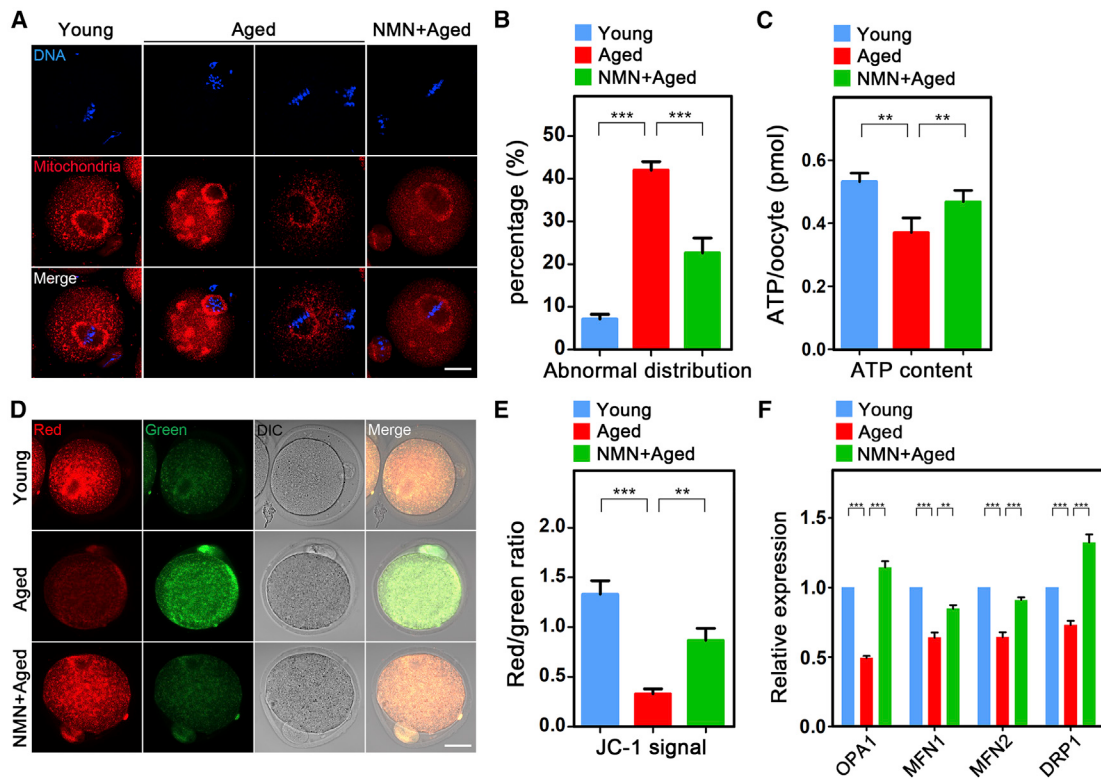


Figure 6. Effect of NMN Supplementation on Mitochondrial Distribution and Function in Aged Oocytes

(A) Representative images of mitochondrial distribution in young, aged, and NMN+aged oocytes. Oocytes were stained with MitoTracker Red to show mitochondria. Scale bar, 20 μ m.

(B) The abnormal rate of mitochondrial distribution was recorded in young ($n = 24$), aged ($n = 17$), and NMN+aged ($n = 15$) oocytes.

(C) ATP levels were measured in young ($n = 30$), aged ($n = 30$), and NMN+aged ($n = 30$) oocytes.

(D) Mitochondrial membrane potential ($\Delta\Psi_m$) was detected by JC-1 staining in young, aged, and NMN+aged oocytes (red, high $\Delta\Psi_m$; green, low $\Delta\Psi_m$). Scale bar, 20 μ m.

(E) The ratio of red to green fluorescence intensity was calculated in young ($n = 14$), aged ($n = 11$), and NMN+aged ($n = 12$) oocytes.

(F) Expression of *Opa1*, *Mfn1*, *Mfn2*, and *Drp1* was examined by RT-PCR in young, aged, and NMN+aged oocytes.

Data in (B), (C), (E), and (F) are presented as mean percentage (mean \pm SEM) of at least three independent experiments. ** $p < 0.01$, *** $p < 0.001$.

NMN Supplementation Attenuates ROS Levels to Suppress DNA Damage and Apoptosis in Aged Oocytes

It is known that mitochondrial dysfunction is a cause of ROS generation and oxidative stress; thus, we carried out dichlorofluorescein (DCFH) staining to compare ROS levels among each group of oocytes. Fluorescence imaging and intensity measurements displayed that much stronger ROS signals appeared in aged oocytes than in young ones (Figures 7A and 7B). On the contrary, NMN supplementation effectively reduced accumulated ROS present in aged oocytes (Figures 7A and 7B). Because high levels of ROS usually result in accumulation of DNA damage and apoptosis (Ozben, 2007; Ratan et al., 1994), we next detected the DNA damage by γ -H2A.X staining and apoptosis by Annexin-V staining in young, aged, and NMN+aged oocytes. As we hypothesized, maternal aging led to a higher incidence of DNA damage and apoptosis in oocytes, which was suppressed by supplementation with NMN (Figures 7C–7F). This was consistent with the above observation that reduced $\Delta\Psi_m$, considered a key indicator of apoptosis, could be restored by NMN in aged oocytes. Notably, we demonstrated that the increase in intracellular

ROS levels by H_2O_2 treatment in young oocytes phenocopied aging-induced meiotic defects, such as failed oocyte maturation, aberrant spindle/chromosome structure, and aneuploidy (Figure S6). In addition, we showed that NMN supplementation also ameliorated the maternal aging-induced high levels of ROS, accumulation of DNA damage, and apoptosis in granulosa cells (Figure S7), which might further alleviate apoptosis of oocytes.

DISCUSSION

In mammals, NAD⁺ is a cofactor of various key enzymes that have diverse physiological functions in glycolysis, the tricarboxylic acid cycle, and oxidative phosphorylation, involved in multiple redox reactions in cells (Camacho-Pereira et al., 2016). It has been reported that an age-dependent decrease in NAD⁺ occurs in multiple organs, such as the brain, muscle, pancreas, adipose tissue, and skin, leading to age-related diseases (Das et al., 2018; de Picciotto et al., 2016). NMN, a product of the NAMPT reaction and a key NAD⁺ intermediate (Yoshino et al., 2011), has a crucial role in maintaining the balance of

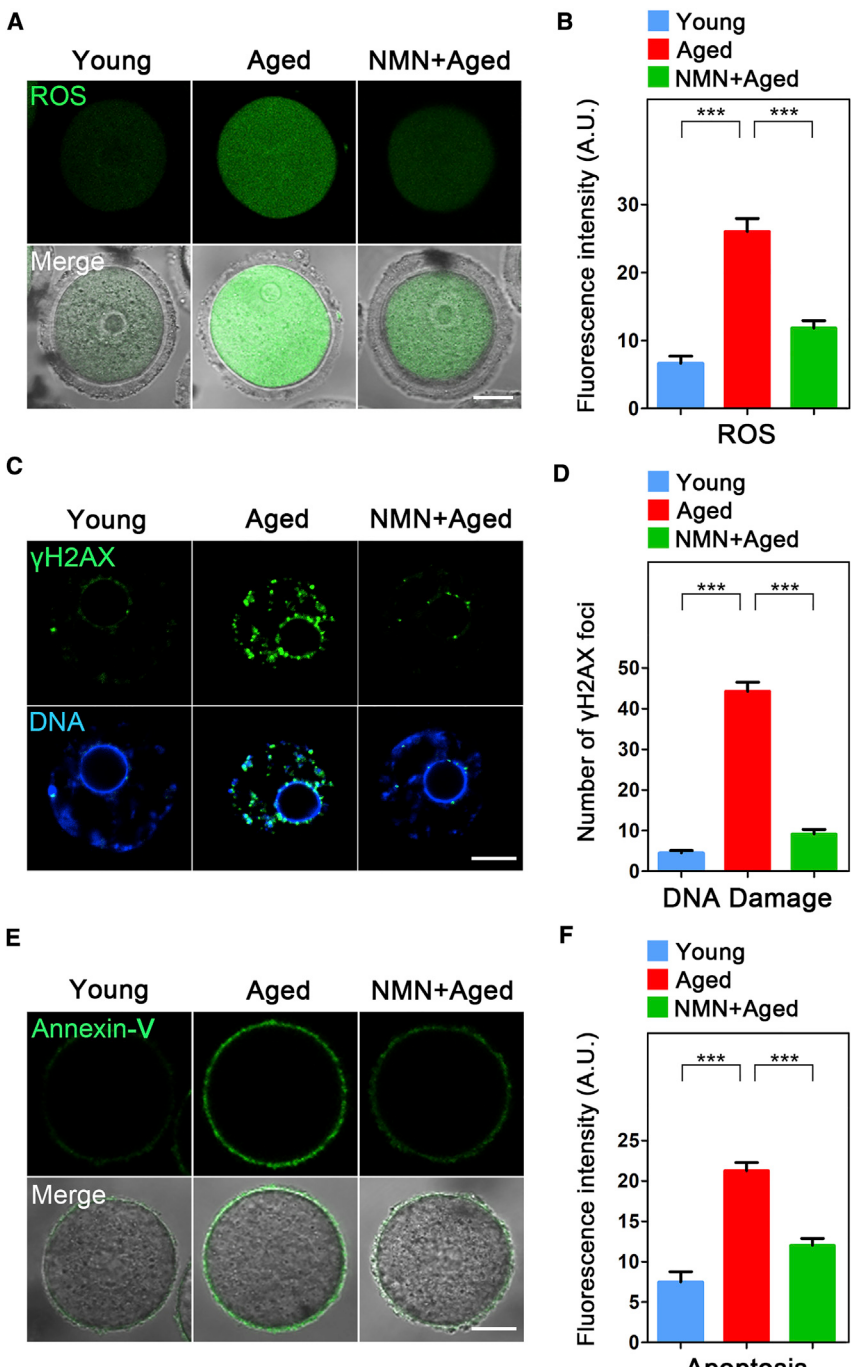


Figure 7. Effect of NMN Supplementation on ROS Accumulation, DNA Damage, and Apoptosis in Aged Oocytes

(A) Representative images of ROS levels detected by DCFH staining in young, aged, and NMN+aged oocytes. Scale bar, 20 μ m.

(B) The fluorescence intensity of ROS signals was measured in young ($n = 24$), aged ($n = 21$), and NMN+aged ($n = 23$) oocytes.

(C) Representative images of DNA damage stained with the γ H2AX antibody in young, aged, and NMN+aged oocytes. Scale bar, 10 μ m.

(D) γ H2AX foci were counted in young ($n = 13$), aged ($n = 13$), and NMN+aged ($n = 11$) oocytes.

(E) Representative images of apoptotic status, assessed by Annexin-V staining, in young, aged, and NMN+aged oocytes. Scale bar, 20 μ m.

(F) The fluorescence intensity of Annexin-V signals was measured in young ($n = 16$), aged ($n = 14$), and NMN+aged ($n = 14$) oocytes.

Data in (B), (D), and (F) are presented as mean percentage (mean \pm SEM) of at least three independent experiments. *** $p < 0.001$.

In the present study, we found that the NAD⁺ level was also decreased in oocytes from maternally aged mice but could be recovered by *in vivo* administration of NMN. We then wanted to find out whether restoration of NAD⁺ content by NMN supplementation would ameliorate the low quality of aged oocytes. Consistent with previous studies by us and others (Wu et al., 2019), our findings validated that maternal aging severely impaired follicle development, ovulation, and oocyte maturation. As anticipated, NMN supplementation to some extent increased the number of antral follicles, ovulated oocytes, and matured oocytes with less fragmentation, offering a potentially effective approach to improving the fertility of aged females or acquiring more high-quality oocytes for assisted reproductive technology (ART). We further discovered that NMN elevated the maturation rate of aged oocytes by promoting nuclear and cytoplasmic maturation. NMN supplementation recovered the spindle/chromosome structure and kinetochore-microtubule attachment to maintain

euploidy and nuclear maturation of aged oocytes. Moreover, NMN supplementation restored cytoplasmic maturation of aged oocytes by ensuring normal dynamics of CGs and their component ovastacin, strengthening the sperm binding ability and fertilization capacity of aged oocytes. Consequently, early embryonic development was also boosted.

To ascertain the mechanisms of how NMN improves the quality of aged oocytes, we applied single-cell transcriptome profiling to identify potential target effectors. In line with a previous report

NAD⁺ content in cells (Gomes et al., 2013; Yoshino et al., 2011). NMN is synthesized via two major pathways: (1) nicotinamide (NAM) catalyzes synthesis by NAMPT, and (2) nicotinamide riboside (NR) catalyzes synthesis by NR kinases (NRKs) (Verdin, 2015). Accumulating evidence has shown that enhancing NAD⁺ biosynthesis by treatment with NMN in aged mice reverses age-related dysfunction in multiple organs, including the eyes (Mills et al., 2016), skeletal muscle (Gomes et al., 2013), and peripheral arteries (Das et al., 2018; de Picciotto et al., 2016).

([Tarantini et al., 2019](#)), our findings revealed that genes related to the mitochondrial membrane part, mitochondrial respiratory chain, viral infection, and oxidative phosphorylation pathways were misexpressed in aged oocytes but recovered following NMN supplementation, suggesting that the effect of NMN on aged oocytes might be mediated by mitochondrial function. This supports the notion that aging disrupts mitochondrial function in a variety of cells ([Ham and Raju, 2017](#); [Kiss et al., 2020](#)), and subsequent analyses of mitochondrial distribution, ATP content, and $\Delta\Psi_m$ demonstrated that NMN can reverse mitochondrial dysfunction induced by aging in oocytes.

Reduced $\Delta\Psi_m$ and compromised mitochondrial function predict accumulation of ROS and apoptosis in aged oocytes, which accounts for their high frequency of fragmentation. Our data showed that NMN supplementation efficiently eliminated excessive ROS to suppress DNA damage and apoptosis.

Collectively, we provide *in vivo* evidence documenting that NMN supplementation recovers the NAD⁺ level to improve the quality of maternally aged oocytes by promoting nuclear and cytoplasmic maturation to maintain euploidy and fertilization ability. In particular, NMN restores mitochondrial function of aged oocytes to suppress accumulation of ROS and DNA damage, reducing apoptosis. Interestingly, a recent work reported a similar finding, showing that supplementation of NMN in drinking water for 4 weeks prominently rejuvenated oocyte quality and restored the fertility of aged mice ([Bertoldo et al., 2020](#)). They further indicated that Sirt2 overexpression recapitulated the benefits of NMN treatment ([Bertoldo et al., 2020](#)). Our data validated that Sirt1 was also implicated in the effects of NMN on aged oocytes. Overall, our work expounds a theoretical basis for application of NMN to improve the fertility of aged women and the efficiency of ART.

STAR★METHODS

Detailed methods are provided in the online version of this paper and include the following:

- **KEY RESOURCES TABLE**
- **RESOURCE AVAILABILITY**
 - Lead Contact
 - Materials Availability
 - Data and Code Availability
- **EXPERIMENTAL MODEL AND SUBJECT DETAILS**
 - Mice
- **METHOD DETAILS**
 - Measurement of NAD⁺ levels
 - Oocyte collection and *in vitro* maturation
 - Histological analysis of ovaries
 - Immunofluorescence and confocal microscopy
 - Chromosome spreading
 - Immunoblotting analysis
 - Sperm binding assay
 - *In vitro* fertilization and embryo culture
 - Single-cell RNA library construction and transcriptome sequencing
 - RNA isolation and quantitative real-time PCR
 - Evaluation of total ATP content

● QUANTIFICATION AND STATISTICAL ANALYSIS

- Statistical analysis

SUPPLEMENTAL INFORMATION

Supplemental Information can be found online at <https://doi.org/10.1016/j.celrep.2020.107987>.

ACKNOWLEDGMENTS

We thank Dr. Jurrien Dean for providing antibodies. This work was supported by the National Key Research and Development Program of China (2018YFC1004002 and 2018YFC1003802), the National Natural Science Foundation of China (31822053 and 31900592), the Natural Science Foundation of Jiangsu Province (BK20190526), and the China Postdoctoral Science Foundation (2019M651849).

AUTHOR CONTRIBUTIONS

B.X. designed the research. Y.M., Z.C., and Q.G. performed the experiments. Y.M. and B.X. analyzed the data. Y.M., R.R., and B.X. wrote the manuscript.

DECLARATION OF INTERESTS

The authors declare no competing interests.

Received: February 21, 2020

Revised: June 3, 2020

Accepted: July 13, 2020

Published: August 4, 2020

REFERENCES

- Ben-Meir, A., Burstein, E., Borrego-Alvarez, A., Chong, J., Wong, E., Yavorska, T., Naranian, T., Chi, M., Wang, Y., Bentov, Y., et al. (2015). Coenzyme Q10 restores oocyte mitochondrial function and fertility during reproductive aging. *Aging Cell* **14**, 887–895.
- Bertoldo, M.J., Listijono, D.R., Ho, W.J., Riepsamen, A.H., Goss, D.M., Richerni, D., Jin, X.L., Mahbub, S., Campbell, J.M., Habibalahi, A., et al. (2020). NAD(+) Repletion Rescues Female Fertility during Reproductive Aging. *Cell Rep.* **30**, 1670–1681.e7.
- Bonkowski, M.S., and Sinclair, D.A. (2016). Slowing ageing by design: the rise of NAD⁺ and sirtuin-activating compounds. *Nat. Rev. Mol. Cell Biol.* **17**, 679–690.
- Camacho-Pereira, J., Tarragó, M.G., Chini, C.C.S., Nin, V., Escande, C., Warner, G.M., Puranik, A.S., Schoon, R.A., Reid, J.M., Galina, A., and Chini, E.N. (2016). CD38 Dictates Age-Related NAD Decline and Mitochondrial Dysfunction through an SIRT3-Dependent Mechanism. *Cell Metab.* **23**, 1127–1139.
- Cantó, C., Houtkooper, R.H., Pirinen, E., Youn, D.Y., Oosterveer, M.H., Cen, Y., Fernandez-Marcos, P.J., Yamamoto, H., Andreux, P.A., Cettour-Rose, P., et al. (2012). The NAD(+) precursor nicotinamide riboside enhances oxidative metabolism and protects against high-fat diet-induced obesity. *Cell Metab.* **15**, 838–847.
- Ciancimino, L., Laganà, A.S., Chiofalo, B., Granese, R., Grasso, R., and Triolo, O. (2014). Would it be too late? A retrospective case-control analysis to evaluate maternal-fetal outcomes in advanced maternal age. *Arch. Gynecol. Obstet.* **290**, 1109–1114.
- Combelles, C.M., and Albertini, D.F. (2003). Assessment of oocyte quality following repeated gonadotropin stimulation in the mouse. *Biol. Reprod.* **68**, 812–821.
- Croteau, D.L., Fang, E.F., Nilsen, H., and Bohr, V.A. (2017). NAD⁺ in DNA repair and mitochondrial maintenance. *Cell Cycle* **16**, 491–492.
- Das, A., Huang, G.X., Bonkowski, M.S., Longchamp, A., Li, C., Schultz, M.B., Kim, L.J., Osborne, B., Joshi, S., Lu, Y., et al. (2018). Impairment of an

- Endothelial NAD(+)–H₂S Signaling Network Is a Reversible Cause of Vascular Aging. *Cell* 173, 74–89.e20.
- de Picciotto, N.E., Gano, L.B., Johnson, L.C., Martens, C.R., Sindler, A.L., Mills, K.F., Imai, S., and Seals, D.R. (2016). Nicotinamide mononucleotide supplementation reverses vascular dysfunction and oxidative stress with aging in mice. *Aging Cell* 15, 522–530.
- Duong, H.T., Hoyt, A.T., Carmichael, S.L., Gilboa, S.M., Canfield, M.A., Case, A., McNeese, M.L., and Waller, D.K.; National Birth Defects Prevention Study (2012). Is maternal parity an independent risk factor for birth defects? *Birth Defects Res. A Clin. Mol. Teratol.* 94, 230–236.
- Eijkemans, M.J., van Poppel, F., Habbema, D.F., Smith, K.R., Leridon, H., and te Velde, E.R. (2014). Too old to have children? Lessons from natural fertility populations. *Hum. Reprod.* 29, 1304–1312.
- Gomes, A.P., Price, N.L., Ling, A.J., Moslehi, J.J., Montgomery, M.K., Rajman, L., White, J.P., Teodoro, J.S., Wrann, C.D., Hubbard, B.P., et al. (2013). Declining NAD(+) induces a pseudohypoxic state disrupting nuclear-mitochondrial communication during aging. *Cell* 155, 1624–1638.
- Ham, P.B., 3rd, and Raju, R. (2017). Mitochondrial function in hypoxic ischemic injury and influence of aging. *Prog. Neurobiol.* 157, 92–116.
- Heffner, L.J. (2004). Advanced maternal age—how old is too old? *N. Engl. J. Med.* 351, 1927–1929.
- Hou, X., Zhu, S., Zhang, H., Li, C., Qiu, D., Ge, J., Guo, X., and Wang, Q. (2019). Mitofusin1 in oocyte is essential for female fertility. *Redox Biol.* 21, 101110.
- Kennedy, B.E., Sharif, T., Martell, E., Dai, C., Kim, Y., Lee, P.W., and Gujar, S.A. (2016). NAD⁺ salvage pathway in cancer metabolism and therapy. *Pharmacol. Res.* 114, 274–283.
- Kiss, T., Nyúl-Tóth, Á., Balasubramanian, P., Tarantini, S., Ahire, C., Yabluchanskiy, A., Csipo, T., Farkas, E., Wren, J.D., Garman, L., et al. (2020). Nicotinamide mononucleotide (NMN) supplementation promotes neurovascular rejuvenation in aged mice: transcriptional footprint of SIRT1 activation, mitochondrial protection, anti-inflammatory, and anti-apoptotic effects. *Geroscience* 42, 527–546.
- Magnus, M.C., Wilcox, A.J., Morken, N.H., Weinberg, C.R., and Häberg, S.E. (2019). Role of maternal age and pregnancy history in risk of miscarriage: prospective register based study. *BMJ* 364, i869.
- Mills, K.F., Yoshida, S., Stein, L.R., Grozio, A., Kubota, S., Sasaki, Y., Redpath, P., Migaud, M.E., Apte, R.S., Uchida, K., et al. (2016). Long-Term Administration of Nicotinamide Mononucleotide Mitigates Age-Associated Physiological Decline in Mice. *Cell Metab.* 24, 795–806.
- Ozben, T. (2007). Oxidative stress and apoptosis: impact on cancer therapy. *J. Pharm. Sci.* 96, 2181–2196.
- Pantazi, E., Zaouali, M.A., Bejaoui, M., Folch-Puy, E., Ben Abdennabi, H., Varela, A.T., Rolo, A.P., Palmeira, C.M., and Roselló-Catafau, J. (2015). Sirtuin 1 in rat orthotopic liver transplantation: an IGL-1 preservation solution approach. *World J. Gastroenterol.* 21, 1765–1774.
- Park, J.H., Long, A., Owens, K., and Kristian, T. (2016). Nicotinamide mononucleotide inhibits post-ischemic NAD(+) degradation and dramatically ameliorates brain damage following global cerebral ischemia. *Neurobiol. Dis.* 95, 102–110.
- Ratan, R.R., Murphy, T.H., and Baraban, J.M. (1994). Oxidative stress induces apoptosis in embryonic cortical neurons. *J. Neurochem.* 62, 376–379.
- Scheibye-Knudsen, M., Mitchell, S.J., Fang, E.F., Iyama, T., Ward, T., Wang, J., Dunn, C.A., Singh, N., Veith, S., Hasan-Olive, M.M., et al. (2014). A high-fat diet and NAD(+) activate Sirt1 to rescue premature aging in cockayne syndrome. *Cell Metab.* 20, 840–855.
- Schneider, C.A., Rasband, W.S., and Eliceiri, K.W. (2012). NIH Image to ImageJ: 25 years of image analysis. *Nat. Methods* 9, 671–675.
- Tan, T.Y., Lau, S.K., Loh, S.F., and Tan, H.H. (2014). Female ageing and reproductive outcome in assisted reproduction cycles. *Singapore Med. J.* 55, 305–309.
- Tarantini, S., Valcarcel-Ares, M.N., Toth, P., Yabluchanskiy, A., Tucsek, Z., Kiss, T., Hertelendy, P., Kinter, M., Ballabh, P., Süle, Z., et al. (2019). Nicotinamide mononucleotide (NMN) supplementation rescues cerebromicrovascular endothelial function and neurovascular coupling responses and improves cognitive function in aged mice. *Redox Biol.* 24, 101192.
- Verdin, E. (2015). NAD⁺ in aging, metabolism, and neurodegeneration. *Science* 350, 1208–1213.
- Wu, X., Hu, F., Zeng, J., Han, L., and Wang, Q. (2019). NMNAT2-mediated NAD⁺ generation is essential for quality control of aged oocytes. *Aging Cell* 18, e12955.
- Yamaguchi, S., and Yoshino, J. (2017). Adipose tissue NAD(+) biology in obesity and insulin resistance: From mechanism to therapy. *Bioessays* 39.
- Yamamoto, T., Iwata, H., Goto, H., Shiratuki, S., Tanaka, H., Monji, Y., and Kuwayama, T. (2010). Effect of maternal age on the developmental competence and progression of nuclear maturation in bovine oocytes. *Mol. Reprod. Dev.* 77, 595–604.
- Yoshino, J., Mills, K.F., Yoon, M.J., and Imai, S. (2011). Nicotinamide mononucleotide, a key NAD(+) intermediate, treats the pathophysiology of diet- and age-induced diabetes in mice. *Cell Metab.* 14, 528–536.

STAR★METHODS

KEY RESOURCES TABLE

REAGENT or RESOURCE	SOURCE	IDENTIFIER
Antibodies		
Mouse monoclonal anti- α -Tubulin-FITC	Sigma-Aldrich	Cat# F2168; RRID: AB_2827403
Rabbit monoclonal anti-SirT1	Cell Signaling Technology	Cat# 9475; RRID: AB_2617130
Human anti-Centromere	Antibodies Incorporated	Cat# 15-234; RRID: AB_2687472
Rabbit monoclonal anti-Phospho-Histone H2A.X	Cell Signaling Technology	Cat# 9718; RRID: AB_2118009
Rabbit polyclonal anti-mouse Ovastacin	Gift from Dr. Jurrien Dean lab	N/A
Rat monoclonal anti-mouse ZP2	Gift from Dr. Jurrien Dean lab	N/A
Mouse monoclonal anti-Gapdh	Proteintech	Cat# 60004-1-Ig; RRID: AB_2107436
Goat anti-rabbit IgG (H+L), Alexa Fluor 488	ThermoFisher Scientific	Cat# A-11008; RRID: AB_143165
Donkey anti-rabbit IgG (H+L), Alexa Fluor 594	ThermoFisher Scientific	Cat# A-21207; RRID: AB_141637
Donkey anti-mouse IgG (H+L), Alexa Fluor 594	ThermoFisher Scientific	Cat# A-21203; RRID: AB_2535789
Goat anti-human IgG (H+L), Alexa Fluor 555	ThermoFisher Scientific	Cat# A-21433; RRID: AB_2535854
Horse anti-mouse IgG, HRP	Cell Signaling Technology	Cat# 7076; RRID: AB_330924
Goat anti-rat IgG, HRP	Cell Signaling Technology	Cat# 7077; RRID: AB_10694715
Goat anti-rabbit IgG, HRP	Cell Signaling Technology	Cat# 7074; RRID: AB_2099233
Chemicals, Peptides, and Recombinant Proteins		
Nicotinamide mononucleotide	Sigma-Aldrich	Cat# N3501
M2 medium	Sigma-Aldrich	Cat# M7167
M16 medium	Sigma-Aldrich	Cat# M7292
Albumin from bovine serum	Sigma-Aldrich	Cat# A1933
Mineral oil	Sigma-Aldrich	Cat# M8410
Triton X-100	Sigma-Aldrich	Cat# V900502
Tween 20	Sigma-Aldrich	Cat# V900548
Phalloidin-TRITC	Sigma-Aldrich	Cat# P1951
Lens Culinaris Agglutinin (LCA)-FITC	ThermoFisher Scientific	Cat# L32475
Phosphate-buffered saline	ThermoFisher Scientific	Cat# 20012027
Hoechst 33342	ThermoFisher Scientific	Cat# H3570
Propidium iodide	ThermoFisher Scientific	Cat# P3566
NuPAGE LDS Sample Buffer (4X)	ThermoFisher Scientific	Cat# NP0007
EmbryoMax Human Tubal Fluid (HTF) medium	Millipore	Cat# MR-070-D
EmbryoMax KSOM medium	Millipore	Cat# MR-106-D
Hydrogen peroxide solution	Millipore	Cat# 88597
PrimeScript RT master mix	Takara	Cat# RR036A
4% paraformaldehyde	Santa Cruz Biotechnology	Cat# 281692
EX527	MedChemExpress	Cat# HY-15452
Pregnant mare's serum gonadotropin (PMSG)	Jianchun (Nanjing, China)	Cat# A006
Human chorionic gonadotropin (HCG)	Jianchun (Nanjing, China)	Cat# A001-2

(Continued on next page)

Continued

REAGENT or RESOURCE	SOURCE	IDENTIFIER
Critical Commercial Assays		
NAD/NADH Quantification Kit	Sigma-Aldrich	Cat# MAK037
Adenosine 5'-triphosphate (ATP)	Sigma-Aldrich	Cat# FLASC
Bioluminescent Somatic Cell Assay Kit		
MitoTracker Red CMXRos	ThermoFisher Scientific	Cat# M7512
MitoProbe JC-1 Assay Kit	ThermoFisher Scientific	Cat# M34152
Pierce ECL Plus Western Blotting Substrate	ThermoFisher Scientific	Cat# 32132
SYBR Green PCR Master Mix	ThermoFisher Scientific	Cat# 4344463
RNeasy Mini Kit	QIAGEN	Cat# 74104
Annexin V-FITC Apoptosis Detection Kit	Beyotime (Hangzhou, China)	Cat# C1062
Reactive Oxygen Species Detection Kit	Jiancheng (Nanjing, China)	Cat# E004
Experimental Models: Organisms/Strains		
ICR mice	Animal Core Facility of Nanjing Medical University	N/A
Oligonucleotides		
See Table S1 for qPCR primers	This paper	N/A
Software and Algorithms		
ZEN	Carl Zeiss	https://www.zeiss.co.jp/microscopy/ products/microscopesoftware/zen.html
ImageJ	Schneider et al., 2012	https://imagej.nih.gov/ij/
GraphPad Prism 6	GraphPad Software Inc	https://www.graphpad.com/
Other		
Glass slide	Citoglas	Cat# 7105P
PVDF transfer membrane	Bio-Rad	Cat# 1620177

RESOURCE AVAILABILITY

Lead Contact

Requests for further information and resources can be directed to the Lead Contact, Bo Xiong (xiongbo@njau.edu.cn).

Materials Availability

This study did not generate new unique reagents.

Data and Code Availability

Transcriptome data are available in the supplemental tables.

EXPERIMENTAL MODEL AND SUBJECT DETAILS

Mice

All mice were handled in accordance with the Animal Research Institute Committee guidelines of Nanjing Agricultural University, China. The young (6~8-week-old) and aged (64~68-week-old) ICR female mice were kept at controlled condition of temperature (20~23°C) and illumination (12 h light-dark cycle), and had free access to food and water throughout the period of the study. For the aged group, female mice were normally bred with males from 4~6-week-old to 32~34-week-old and then raised to 64~68-week-old. Aged mice were intraperitoneally injected daily with NMN (200 mg/kg body weight per day) or the equivalent volume of PBS for 10 consecutive days. During the collection of oocytes, mice were treated humanely and with regard for alleviation of suffering.

METHOD DETAILS

Measurement of NAD⁺ levels

NAD⁺ levels were measured with a NAD/NADH Quantitation Kit according to the manufacturer's instruction. In brief, 80 oocytes were harvested for total NAD⁺ extraction and quantification based on the procedure described by [Pantazi et al. \(2015\)](#). The NAD⁺

concentration was calculated by subtracting the NADH values from NAD_{total} (NAD⁺ and NADH). NAD_{total} and NADH levels were quantified in a colorimetric assay at 450 nm using iMark™ Microplate Absorbance Reader (Bio-Rad, Hercules, CA, USA).

Oocyte collection and *in vitro* maturation

To collect fully grown GV oocytes, female mice were injected with 5 IU pregnant mare serum gonadotropin (PMSG). After 48 h, cumulus-oocyte complexes were obtained by manually rupturing antral ovarian follicles. Cumulus cells were removed by repeatedly mouth pipetting. For *in vitro* maturation, GV oocytes were cultured in M16 medium at 37°C in an atmosphere of 5% CO₂ for 12 h. To collect ovulated oocytes, female mice received an injection of 10 IU human chorionic gonadotropin (hCG) 48 h after PMSG priming. Oocytes were recovered from oviductal ampullae 13.5 h after hCG, and cumulus cells were removed by a brief incubation in 1 mg/ml hyaluronidase.

Histological analysis of ovaries

Ovaries used for histological analysis were collected from each group of mice and fixed in 4% paraformaldehyde (pH 7.5) overnight at 4°C, dehydrated, and embedded in paraffin. Paraffin-embedded ovaries were sectioned at a thickness of 8 µm for hematoxylin and eosin (H&E) staining. Both ovaries from three mice of each group were used for the analysis.

Immunofluorescence and confocal microscopy

Oocytes were fixed in 4% paraformaldehyde in PBS (pH 7.4) for 30 min and permeabilized in 0.5% Triton X-100 for 20 min at room temperature. Then, oocytes were blocked with 1% BSA-supplemented PBS for 1 h and incubated with anti- α -tubulin-FITC antibody (1:200), anti-centromere antibody (1:200), anti-ovastacin antibody (1:100), anti- γ -H2A.X antibody (1:100), LCA-FITC (1:100) or phalloidin-TRITC (1:100) at 4°C overnight. After washing in PBST, oocytes were incubated with Alexa Fluor 488-conjugated goat anti-rabbit IgG (H+L), Alexa Fluor 594-conjugated donkey anti-rabbit IgG (H+L), Alexa Fluor 594-conjugated donkey anti-mouse IgG (H+L) or Alexa Fluor 555-conjugated goat anti-human IgG (H+L) for 1 h at room temperature. Then oocytes were counterstained with Hoechst for 10 min. Finally, oocytes were mounted on glass slides and observed under a laser scanning confocal microscope (LSM 700, Carl Zeiss).

For active mitochondrion staining, oocytes were cultured in M16 medium containing 500 nM cell permeant MitoTracker Red CMXRos for 30 min at 37°C in a dark environment and 5% CO₂ in air. After washing three times with fresh M2 medium for 20 min each, oocytes were mounted on non-fluorescent glass slides and observed under the laser scanning confocal microscope.

Mitochondrial membrane potential was evaluated using MitoProbe JC-1 Assay Kit. Briefly, oocytes were cultured in M16 medium with 2 µM JC-1 for 30 min at 37°C, followed by washing with buffer for 10 min. Samples were immediately imaged in a glassbottom dish under the laser scanning confocal microscope. JC-1 dye exhibits potential-dependent accumulation in mitochondria, indicated by a fluorescence emission shift from green (~529 nm) to red (~590 nm). Thus, mitochondrial depolarization is indicated by a decrease in the red/green fluorescence intensity ratio.

For DCFH staining, oocytes or granulosa cells were incubated with the oxidation-sensitive fluorescent probe [dichlorofluorescein (DCFH)] for 30 min at 37°C in DPBS that contained 10 µM DCFH diacetate (DCFHDA). Then oocytes were washed three times in DPBS containing 0.1% BSA and placed on glass slides and observed under the laser scanning confocal microscope.

For Annexin-V staining, oocytes or granulosa cells were stained with the Annexin-V Staining Kit according to the manufacturer's instruction. After washing twice in PBS, the viable oocytes were stained for 30 min in the dark with 90 µL of binding buffer containing 10 µL of Annexin-V-FITC. Then oocytes were washed three times in DPBS containing 0.1% BSA and placed on glass slides and observed under the laser scanning confocal microscope.

For the measurement of fluorescence intensity, signals from both control and treatment oocytes were acquired by performing the same immunostaining procedure and setting up the same parameters as those used with the confocal microscope. ImageJ (NIH, Bethesda, MD, USA) was used to define a region of interest (ROI), and the average fluorescence intensity per unit area within the ROI was determined. The average values of all measurements were used to compare the final average intensities between the control and treatment groups.

Chromosome spreading

Oocytes were incubated in Tyrode's buffer (pH 2.5) for about 30 s at 37°C to remove zona pellucida. After recovery in M2 medium for 10 min, oocytes were fixed in a drop of 1% paraformaldehyde with 0.15% Triton X-100 on a glass slide. After air drying, chromosomes were counterstained with PI and examined by confocal microscope.

Immunoblotting analysis

Oocytes were lysed in 4 × LDS sample buffer containing protease inhibitor, and then separated on 4%–12% Bis-Tris precast gels and transferred onto PVDF membranes. The blots were blocked in TBST containing 5% low fat dry milk for 1 h at room temperature and then incubated with 1:500 dilution of M2c.2, ovastacin or Sirt1 antibodies overnight at 4°C. After wash in TBST, the blots were incubated with the HRP-conjugated horse anti-mouse IgG, goat anti-rat IgG or goat anti-rabbit IgG for 1 h at room temperature. Chemiluminescence was detected with ECL Plus and protein bands were acquired by Tanon-3900 Chemiluminescence Imaging System.

Sperm binding assay

Caudal epididymal sperm were isolated from wild-type male mice and placed under mineral oil in Human tubal fluid (HTF) medium previously equilibrated with 5% CO₂ and capacitated by an additional 1 h of incubation at 37°C. Sperm binding to ovulated oocytes were observed using capacitated sperm and 2-cell embryos as a negative wash control. Samples were fixed in 4% PFA for 30 min, stained with Hoechst 33342. Bound sperm were quantified from z projections acquired by confocal microscope, and results reflect the mean ± SEM from at least three independently obtained samples.

In vitro fertilization and embryo culture

Caudae epididymides from 12-week-old male mice were lanced in a dish of HTF medium under mineral oil to release sperm, followed by being capacitated for 1 h (37°C, 5% CO₂), and added to ovulated oocytes at a concentration of 4×10^5 /mL sperm in 100 μL HTF for 5 h at 37°C, 5% CO₂. The presence of two pronuclei was scored as successful fertilization. The embryos were cultured in a 96-well culture plate containing 150 μL KSOM under 50 μL mineral oil at 37°C in a 5% CO₂ atmosphere.

Single-cell RNA library construction and transcriptome sequencing

Transcriptomic analysis of matured oocytes was carried out using a protocol for single cell RNA-Seq. In brief, 3 sets of samples were collected for each group (3 oocytes per sample) in lysis buffer. The single cell collection solution contains cell lysis components and RNase inhibitors. The nucleic acid sequence with oligo dT was used for reverse transcription to form the 1st cDNA. The 1st cDNA was amplified by PCR to enrich nucleic acid, and the library was constructed after purification of amplified products, including DNA fragmentation, end repair, adding "A" and joint, PCR amplification and library quality control. The constructed library was sequenced with Illumina platform. The sequencing strategy was PE150. The original down sequence (Raw Reads) obtained from Hiseq sequencing was completed through the process of removing low-quality sequence and connector pollution according to the processing, high-quality sequences (clean reads) were obtained, and all subsequent analysis was based on clean reads.

RNA isolation and quantitative real-time PCR

Total RNA was extracted from a total of 50 oocytes using RNeasy Mini Kit and reversed to cDNA using PrimeScript RT Master Mix, followed by storage at -20°C until use. Quantitative real-time PCR was conducted using SYBR Green PCR Master Mix with Quant-Studio 7 Flex Real-Time PCR System (ThermoFisher, Waltham, MA, USA). Primers were shown in [Table S1](#). Data were normalized against *Gapdh* and quantification of the fold change was determined by the comparative CT method. Experiments were performed at least three times.

Evaluation of total ATP content

Total ATP content in a pool of 10-20 oocytes was determined using the Bioluminescent Somatic Cell Assay Kit, following the procedure described by [Combelles and Albertini \(2003\)](#) and the manufacturer's instruction. A 5-point standard curve (0, 0.1, 0.5, 1.0, 10, and 50 pmol of ATP) was generated in each assay and the ATP content was calculated by using the formula derived from the linear regression of the standard curve.

QUANTIFICATION AND STATISTICAL ANALYSIS

Statistical analysis

All percentages or values from at least three repeated experiments were expressed as mean ± SEM, and the number of oocytes observed was labeled in parentheses as (n). Data were analyzed by paired-samples t test, provided by GraphPad Prism 6 statistical software. The level of significance was accepted as p < 0.05.